

# Electromagnetic Coupling in Near-Field Scattering by Small Homogeneous and Heterogeneous Nanoaggregates

S. Bruzzone,\* M. Malvaldi, G. P. Arrighini, and C. Guidotti

Università degli Studi di Pisa, Dipartimento di Chimica e Chimica Industriale, Via Risorgimento 35, 56100 Pisa Italy

Received: July 13, 2005; In Final Form: October 21, 2005

Progress in near-field optical spectroscopy research on metal nanoparticles demands a better understanding of the role played by particle–particle interactions and a deeper insight of the influence of the incident field wavelength. This is particularly true for scanning near-field optical microscopy (SNOM), where the mechanism by which some components of the evanescent illuminating field are transformed into propagating field components that carry information about the sample is at the core of the image formation and where the role played by the interactions between sample and tip remains a still open problem. In this perspective, we investigate numerically the optical behavior of small aggregates of spherical nanoparticles, taking into account the electromagnetic coupling between all particles and the apertureless tip. The tip is modeled as a sphere made of different materials characterized by appropriate dielectric functions. We find that the tip material affects both qualitatively and quantitatively the SNOM images; more important, from the analysis of the calculated scattering cross section, the resonance plasmon location of the whole (aggregate + tip) system undergoes detectable changes, if the tip is constituted of the same material of the sample, as the tip is situated in different positions. This modification of the plasmon frequencies induces a nontrivial variation of the near-field intensity as a function of the tip position and the resulting SNOM image can be distorted with respect to the actual shape of the sample. No simple arguments can be used to relate the value of the local field on the tip surface to the scattering cross section value; depending on the tip material, the comparison between these two measurements can help to clarify the role of basic interactions in the scattering mechanism.

## Introduction

In recent years, the electromagnetic (em) response of metallic nanoparticles to UV–visible light has become one of the most studied topics in both theoretical and experimental physics.<sup>1–4</sup> Usually, observations carried out in optical scattering experiments are done in the so-called far-field zone, that is, at a great distance from the scattering object compared with both wavelength of the light used and dimensions of the object. Anyway, when the scattering object is composed of close or densely packed subunits, the enhanced field on (or close to) the surface of the particles (which can be of several orders of magnitude larger than the incident field) plays an important role even in the far-field scattering behavior.<sup>5</sup> Such near-field effects can be exploited to analyze the nanometric object that gives rise to them with a spatial resolution much higher than the one achievable by traditional microscopy.

At the moment, the scanning near-field optical microscopy (SNOM) technique<sup>6,7</sup> is one of the most powerful instrumental techniques available, with a wide range of possible applications, such as the study of em interactions on a nanometric scale,<sup>8</sup> the study of nanometric surface-roughness characterization or the quantitative investigation of surface-enhanced spectroscopies.<sup>9</sup> From a theoretical point of view, SNOM has been studied adopting different models and approximations, for example modeling the probe by an electric dipole,<sup>10</sup> assuming a passive role for the probe,<sup>11</sup> or by electrostatic approximation.<sup>12</sup> Anyway,

it is now commonly accepted that the tip–sample interactions play a nonnegligible role in the scattering behavior of the system and consequently in the field intensity measured experimentally.<sup>13</sup>

Despite this, the interpretation of SNOM results can still be not straightforward, considering also that the fundamental interactions involved in the image formation have been neither extensively nor systematically studied. A not negligible amount of theoretical and experimental work is still to be done, to first understand and then fully exploit the capabilities of this technique.

A very important prerogative of SNOM is the fact that by such technique one is allowed to study, through scattered near-field measurements, both the shape and the spatial structure of the induced polarization in the sample.<sup>14</sup> The signal provides more information about one or other of these two aspects depending on the wavelength utilized. Usually excitation wavelengths close to the plasmon resonance are used, because in these experimental conditions the scattering intensity is greatly enhanced. On the other side, induced polarization effects can arise when the exciting wavelength is close to one of the plasmon resonances of the whole (probe+sample) system. Since the spatial structure of the induced polarization can differ markedly from that of the bare sample, a not negligible contribution of this effect (when close to a resonance) can distort the SNOM image of the sample rather than increasing the resolution. Therefore, the signal should be used not to study the shape of the sample, but to explore the local details of the excited plasmons for each resonance frequency.

\* Corresponding author. Telephone: 0039-0502219294. Fax: 0039-0502219260. E-mail: sama@cci.unipi.it.

At the same time, in near-field microscopy techniques, interference phenomena between radiation outcoming from scatterers in different positions can be detected.<sup>15</sup> This effect can be exploited, for instance, for high-resolution distance measurements.

These two effects, coupling and interference, are able in principle to modify the field intensity in a nontrivial way: if, in one sense, both of them affect the SNOM images, relative to the shape of the sample, introducing artifacts, at the same time, they can also be exploited to get information not accessible by other kinds of microscopies. It is important to stress that such aspects are dependent on the wavelength used and on the coupling strength between the particles constituting the sample and the probe. It is well-known, for instance, that the wavelength of the illuminating field affects the intensity of the near-field scattered by a single nanoparticle,<sup>16</sup> because of the strong correlation between plasmon resonances of the scattering object and scattering efficiency. Another confirmed aspect is that the plasmon resonances are a characteristic fingerprint of both shape and dimensions of the scattering object.<sup>17,18</sup> Yet, while there are plenty of studies about the role of size and shape of isolated nanoparticles, it is a noteworthy fact that aggregates of identical nanoparticles usually display plasmon resonances different from that of the single particle, due to strong coupling effects between very close subunits,<sup>5</sup> so that the plasmon resonances of an aggregate can be changed by modifying the position of one or more of its constituents. These possibilities thus should not be neglected in the choice of the experimental wavelength. Although fundamental to understand correctly the scattering behavior of aggregates, this occurrence has received considerably less attention in the past.

In a former work,<sup>19</sup> we proposed a low-cost computational approach (with explicit treatment of quantum size effects) based on a previously developed model<sup>20,21</sup> for the study of the em extinction and scattering by aggregates of spherical particles, in the intent of obtaining some qualitative indications about the role of the scanning probe tip in SNOM experiments. In the present work, we use the same model to investigate to which extent the nature of the material of which the tip probe is built and frequency of the illuminating light can affect the result of an experiment. This problem will be analyzed calculating for two different samples: (i) the near field intensity locally illuminating the tip (as a function of the tip position) and (ii) the scattering cross section spectra, for different positions of the tip and two different samples (see the next sections).

In the next section, the systems studied and the model utilized will be briefly outlined, whereas numerical results and discussion are addressed in sections III and IV.

## Model and Calculations

The results presented in this paper refer to em scattering by small aggregates following the same treatment already discussed in a previous paper.<sup>19</sup> The systems are constituted by identical nanosized Ag particles (sample), lying in the  $xy$  plane, at  $z = 0$ , in the presence of a single particle characterized by appropriate dielectric properties which can be changed to simulate different materials (Ag, Au, or dielectric material). In this simple picture, this additional particle is assumed to represent the probe tip of the SNOM experimental setup, with the center of the tip particle scanning the sample plane  $xy$ , through moves on a grid at a given plane with  $z = z_{\text{tip}}$  (for a clear view of the topological arrangement of the particles involved, see also Figures 1 and 2). We remark that the  $(x,y)$  coordinates of tip-particle center change during each calculation, with the  $z$  coordinate remaining

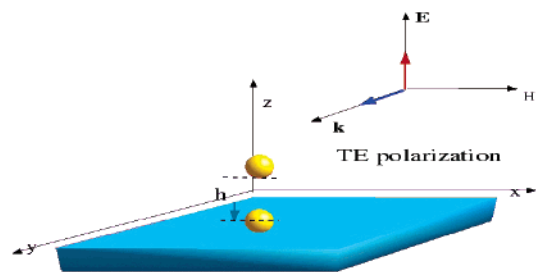


**Figure 1.** Schematic representation of the simulated experimental setup in system 1. The tip probe spans the  $(x,y)$ -plane, at a fixed height  $z_{\text{tip}}$  along the  $z$ -axis. Note that locations, particle, and tip probe radii are not in scale. The spatial arrangement of the fields, in the polarizations adopted, is represented in the lower part of Figure.

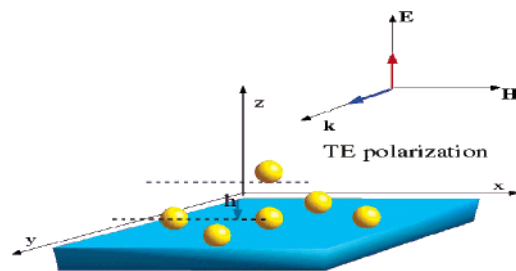


**Figure 2.** Schematic representation of the simulated setup of system 2 (see also caption of Figure 1). The table associated with the figure (Table 1) reports the coordinates of the metal particles in nanometers.

**TABLE 1.**  $(x,y)$ -Coordinates of the Sample Metal Particles in System 2 (see Figure 2)

$x$ (nm)	50	50	50	20	80
$y$ (nm)	50	20	80	50	50

constant at the value  $z = z_{\text{tip}}$ . Our choice to simulate the tip with a spherical nanoparticle is anyway realistic, and in recent years several experiments performed with a single gold nanoparticle as a probe have been reported.<sup>14</sup> The system is illuminated by an incoming plane em wave of wavelength  $\lambda = 415.4$  nm, propagating along the  $y$  axis and with the electric field oriented along the  $z$  direction (this setup of the field is usually referred to as TE polarization). This wavelength has been selected because it lies in proximity of the plasmon resonance of two close Ag nanoparticles of dimension close to the one chosen. The same choice has been made in experimental works,<sup>22</sup> in order to ensure appreciable effects of local field enhancement. At a wavelength corresponding to plasmon resonance, the scattered field by the particles is (close to the surfaces of the particles) much more intense than the incident field. Moreover, the scattered field outcoming from the particles does not have a single polarization direction.<sup>21</sup> The distribution of the polarization of scattered field ensures, as far as the particles are close enough, a detectable amount of coupling, no matter which polarization is the one of the incident field.<sup>23</sup>

The first system studied (system 1) involves a single-particle sample, while in the second system (system 2), the sample is built by five particles arranged as in Figure 2, the corresponding coordinate values being those collected in Table 1. For simplicity, it is assumed that in both cases the systems is embedded in a homogeneous medium (vacuum) and the radius of all particles is chosen equal to  $R = R_{\text{tip}} = 10$  nm.

The material constituting the sample and tip is characterized through the appropriate dielectric function. In the case of metal particles the dielectric behavior takes approximately into account effects related to their dimensions (quantum size effects). The model adopted (noninteracting electron gas confined in a box<sup>24</sup>), despite its simplicity, is able to reproduce correctly the

wavelength dependence of the dielectric function. Conversely, when the metal tip is replaced by one of dielectric material, its dielectric function is assumed to be independent of the wavelength and its value is  $\epsilon = 1.44$ .<sup>25</sup>

For any tip position, we calculate the scattered field intensity  $|\vec{E}_{\text{sc}}|^2$  at the point individuated by the same  $(x,y)$  values as the tip center and  $z$  coordinate corresponding to  $z = h = z_{\text{tip}} - R_{\text{tip}}$  (so that  $(x,y,z)$  refers to the lower surface of the tip). The calculation of the field intensity has been carried out following the very general treatment put forward by Gerardy and Ausloos,<sup>5,20</sup> in terms of a procedure (a generalization of the Mie theory) that involves the solution of Maxwell equations with standard boundary conditions, obtained by expanding the fields scattered by any particle in terms of vector spherical harmonics (the reader is addressed to the original works for any further detail concerning theoretical aspects). Here, it is important to underline that the theory followed is general enough to include even magnetic multipolar orders and the coupling of them to the electric multipoles. In this way, the em coupling between the particles can be given even by high order multipolar effects.

The signal measured in SNOM experiments is assumed to be directly correlated to the near-field em intensity illuminating locally the tip: this is one of the possible physically grounded interpretations of the SNOM signal.<sup>13,26,27</sup> The right quantity to be calculated in order to reproduce the SNOM signal should be the amplitude of the electric field in the position where the detector is located, that is, far from the sample. Such calculation would be subject to heavy numerical errors due to the limited number of multipoles used in the expansion, and an enormous number of multipoles would be required to obtain an acceptable value.<sup>28</sup> Our choice is a strong approximation with the advantage of ensuring fast calculations. A better description of the field distribution around the probe particle would be, for the reason explained above, an approximation indeed which could only slow considerably the calculation speed without significant changes of the results.

In the same framework used for electric field calculations, for few selected positions of the tip particle, the normalized far-field scattering cross section spectra have been calculated. This has been done to study the wavelength dependence of plasmon resonances in the systems and to check the adequacy of our wavelength choice.

## Results and Discussion

As already mentioned, the results presented in this paper refer to two simple systems, of which the first one is constituted by a single spherical Ag particle (center coordinates: (25,25,0) nm) and the second one built by five Ag particles, whose centers are in the positions indicated in Table 1. In each case, the center of the tip particle explores a set of grid points belonging to the plane  $z_{\text{tip}} = R_{\text{tip}} + h = \text{constant}$ , parallel to the  $z = 0$  one, sampling a total of  $51 \times 51$  pairs of  $(x,y)$  values (scanned by 2 nm steps), as reported in Figures 1 and 2. The value of the parameter  $h$  adopted in this work, if not differently specified, is chosen equal to 11 nm, so that between the surface of the tip—particle and surface of sample—particles there is a distance at least equal to 1 nm. In Figure 4, 6, and 7, the value of the parameter  $h$  is varied (from 10.002 to 15 nm) in order to understand the role and importance of the tip—sample distance.

One of the main intents of this work is understanding how and to which extent the em coupling between particles can modify the scattering response of an aggregate. As remarked in several works, involved multipole—multipole coupling effects fades away with increasing interparticle distance. As distances

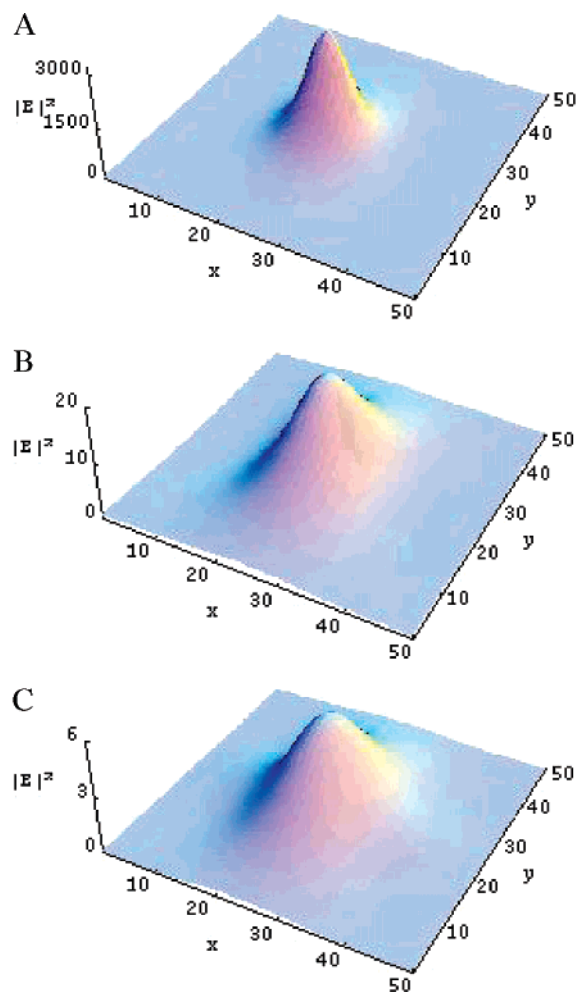


**Figure 3.**  $|\vec{E}_{\text{sc}}(\vec{r})|^2$  plot for different  $(x,y)$  positions of the tip probe ( $R_{\text{tip}} = 10$  nm) scanning the plane at height  $h = z_{\text{tip}} - R_{\text{tip}}$ , for a sample constituted by a single Ag particle (system 1) and for different materials constituting the tip probe. Key: (a) tip made of Ag; (b) tip made of Au; (c) tip made of dielectric material.

become greater than 5 times the sum of the radii of particles, these effects become negligible.<sup>5</sup> For this reason, in system 2, the distances chosen between the particle centers are all equal to 30 nm, to ensure that coupling effects are not ignorable. In addition, two other aspects play a ground role in the em coupling mechanism: the first one is the wavelength chosen for the incident field, which modulates the amplitude of the response, and the second one are the (eventually different) dielectric functions of the interacting particles at the wavelength employed. A detectable interaction is thus expected when, at the wavelength chosen, the particles show a similar (or corresponding) dielectric functions. In this sense, the systems chosen represent different situations; when the tip is constituted of the same material of the sample (Ag), the strongest interaction is given by the tip particle and the sample particle closest to the tip, because of the reduced distance between the surfaces (that can approach themselves up to 1 nm) with respect to the spacing between sample particle surfaces (10 nm). In contrast, when the probe is constituted by a dielectric material, the interaction between the tip particle and the sample is expected (showed by  $Q_{\text{scn}}$ ) to be poor, and the main interactions are those between the sample particles.

The electric near-field intensity detected by the tip in system 1, for three different tip materials, is reported in Figure 3. In each setup the field intensity is enhanced in proximity of the sample particle: however, the “detected” intensity is strongly



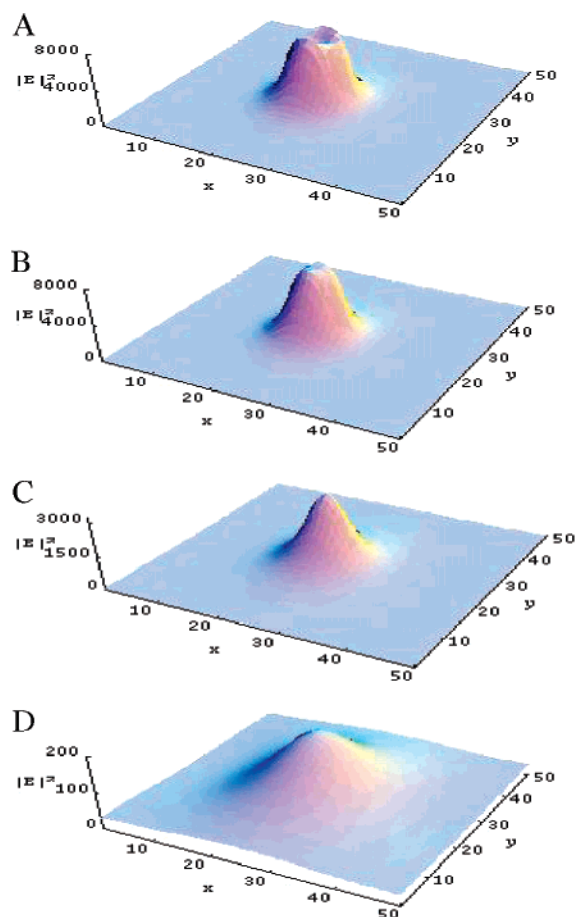


**Figure 4.**  $|\vec{E}_{\text{sca}}(\vec{r})|^2$  plot for different  $(x,y)$  positions of the tip probe ( $R_{\text{tip}} = 10$  nm) made of Ag scanning the plane at different height  $h = z_{\text{tip}} - R_{\text{tip}}$ , for a sample constituted by a single Ag particle (system 1). Key: (a)  $h = z_{\text{tip}} - R_{\text{tip}} = 10.02$  nm; (b)  $h = z_{\text{tip}} - R_{\text{tip}} = 10.2$  nm; (c)  $h = z_{\text{tip}} - R_{\text{tip}} = 11$  nm (analogous to Figure 3a); (d)  $h = z_{\text{tip}} - R_{\text{tip}} = 15$  nm.

dependent on the tip material. Thus, for the dielectric tip (Figure 3c), the field intensity enhancement is less than 1 order of magnitude, while with the Au tip (Figure 3b) a more marked enhancement is observed, which becomes “explosive” when the tip is made of the same material as the sample (Ag, Figure 3a).

The same sample, with a probe made of Ag, has been studied at different heights  $h$  of the tip probe; the results of these calculations are reported in Figure 4. The chosen values for  $h$  goes from 10.002 to 15 nm, where the lowest value represents a limit situation (in which the particles display a very strong coupling) already utilized for similar theoretical studies.<sup>5</sup> As expected, the amplitude of the electric field decreases sensibly as the tip probe is raised, while, due to the lower coupling extent, the shape of the signal changes. In particular, when the height of the tip probe is equal to the maximum value here considered,  $h = 15$  nm, the signal of the single particle of sample is spread out to a greater extent around the particle (Figure 4d), if compared with the calculations with the smaller values of  $h$  (Figure 4a,b,c). However, the most interesting feature of field localization to note is the saddle-shaped structure of the signal in proximity of the alignment point between sample and tip—particle along the  $z$  axis, when the probe height is sufficiently low (less than 0.5 nm). This rather surprising aspect, meaning that the maximum intensity detected by the tip does not correspond to the situation in which the particles are at minimal distance, is related to the variation of the plasmon frequencies as the tip and the sample approach each other.

**TABLE 2.** Scattering Cross Section  $C_{\text{sca}}$  ( $\text{au}^2$ ) for System 1 (Single Ag Particle) for Two Different Positions of the Tip Particle, Where Eclipsed Indicates Tip Coordinates (50, 50, 20) nm, While Staggered Refers to Tip Coordinates (48, 50, 20) nm

	eclipsed	staggered
Ag tip	1742.5	1863.9
Au tip	26.1	25.5
dielectric tip	14.2	14.2

As reported in Table 2, which will be discussed later, the scattering cross section spectrum of the system changes slightly but detectably as the geometry of the system is varied. This in turn means that the scattering efficiency at the chosen wavelength can change in a nonmonotonic fashion (e.g., passing through a maximum or a minimum in the scattering cross section spectra) while the tip particle gets closer to the sample upper surface. To understand this behavior, it must be observed that the variation of the near-field intensity, at a fixed wavelength, depends on the geometry in two different ways. The first one is the expected decay of the scattered field with increasing distance from the particle surface, which results in an enhancement of the field intensity detected when the sample surface is approached by the probe. The second aspect to be considered is the variation of the plasmon resonances with the geometry

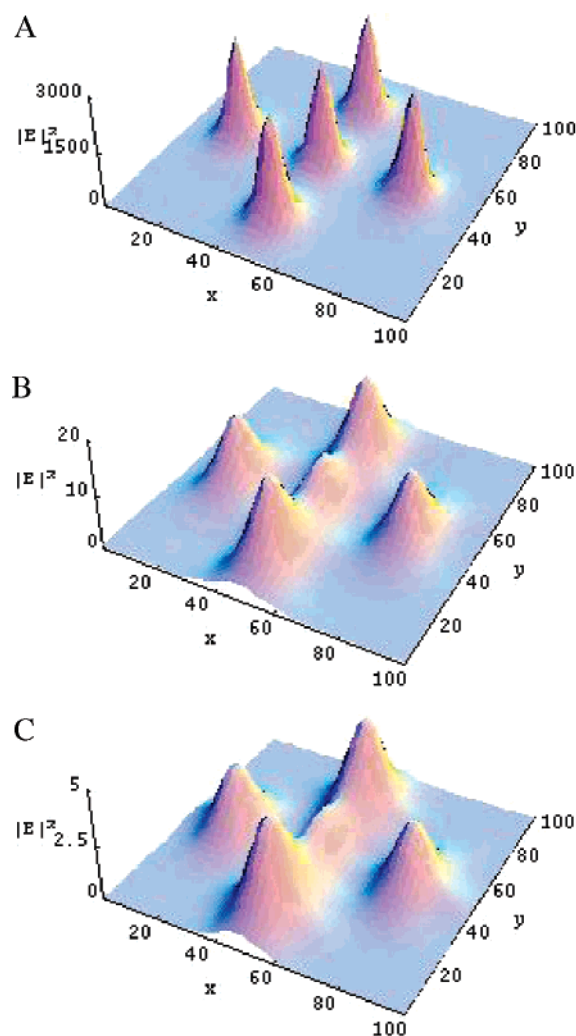


**Figure 5.**  $|\vec{E}_{\text{sca}}(\vec{r})|^2$  plot for different  $(x,y)$  — positions of the tip probe ( $R_{\text{tip}} = 10$  nm) scanning the plane at height  $h = z_{\text{tip}} - R_{\text{tip}}$ , for a sample constituted by 5 Ag particles arranged as reported in Table 1 (system 2), for different materials constituting the tip probe. Key: (a) tip made of Ag; (b) tip made of Au; (c) tip made of dielectric material.

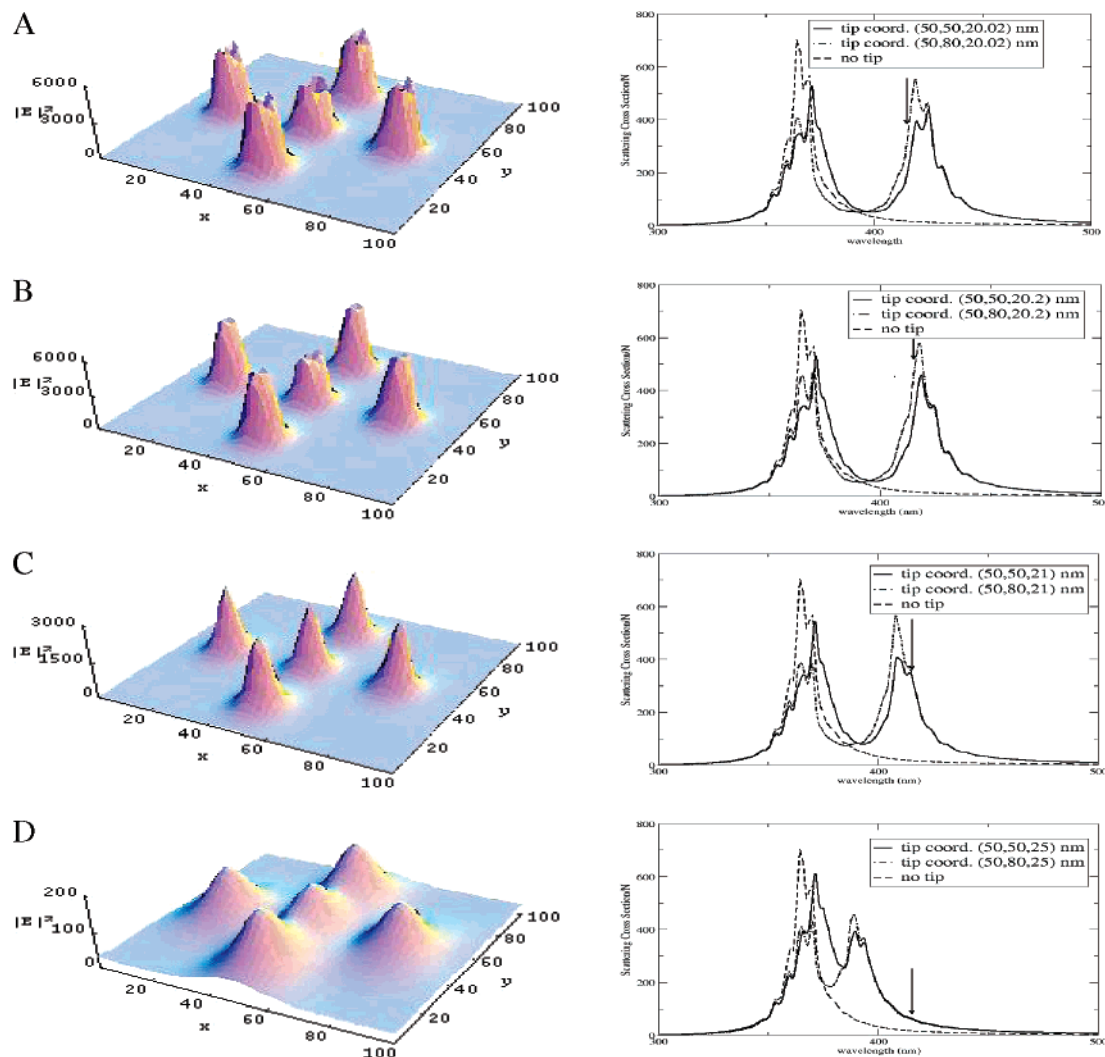


**Figure 6.** Analysis of system 2 with the tip probe ( $R_{\text{tip}} = 10$  nm) made of Ag at different height  $h = z_{\text{tip}} - R_{\text{tip}}$ . Left:  $|\vec{E}_{\text{sca}}(\vec{r})|^2$  plot for different  $(x,y)$  – positions. Right: Scattering cross section  $C_{\text{sca}}$  vs optical wavelength in TE polarization, in absence of the tip particle (dashed line), with Ag tip aligned along the  $z$  axis on the central particle (full line), or with Ag tip aligned along the  $z$  axis on a side particle (dashed–dotted line). The arrow points on the wavelength used for near-field calculations. Key: (a)  $h = z_{\text{tip}} - R_{\text{tip}} = 10.02$  nm; (b)  $h = z_{\text{tip}} - R_{\text{tip}} = 10.2$  nm; (c)  $h = z_{\text{tip}} - R_{\text{tip}} = 11$  nm; (d)  $h = z_{\text{tip}} - R_{\text{tip}} = 15$  nm.

that arises when the two particles are close enough to interact appreciably by their em coupling: in this situation the variation of the scattering intensity at a fixed wavelength is not simply increasing monotonically as the distance is reduced, but depends on the wavelength chosen in a nontrivial fashion. Evidence of this behavior can be found in Table 2 (referred to the system 1), where the values of the evaluated scattering cross section for two different geometries of the setup are reported, at  $\lambda = 415.4$  nm. Here, the “eclipsed” geometry refers to the situation where both particles are aligned along the  $z$  direction, while in the “staggered” geometry the tip particle position is shifted of 2 nm in the  $x$  direction and its center coordinates are (48,50,20.2) nm. Consistently with the behavior previously observed for the electric field intensity, we note that for the Au or dielectric tip–particle, the value of the scattering cross section is essentially unmodified in both geometries. Conversely, for the Ag tip–particle, the scattering cross section is sensibly higher for the staggered geometry. A possible explanation of the saddle-shaped signal observed in Figure 4 can be provided hypothesizing that when the two particles are aligned along the electric field direction, that is, in this case, along  $z$  axis, their coupled longitudinal plasmons are splitted in two eigenmodes, respectively in-phase and out-of-phase. The result is that, when the

distance between the center of the particles is less than 0.5 nm, the field can be reduced, due to destructive interference of the out-of-phase mode. Such mechanism of surface plasmon shift, which was theoretically explored by Quinten and Kreibig,<sup>6</sup> consequently modifies the scattering spectra of the system. The absence of a saddle shape for Au and dielectric tip is thus a consequence of the absence of eigenmode coupling for the two particles due to their different dielectric functions.

A much more revealing evidence of the importance of collective plasmon modification can be seen from the results obtained for system 2, which are presented in Figure 5. In the case of Ag tip probe (Figure 5a), each particle is associated with a well-detectable and resolved signal of comparable intensity for all of them, even if the central sample particle gives a very slightly less intense signal. The effect of suppression of the intensity of the signal when the tip is positioned on the central particle is clearly more prominent when the tip is made of materials other than that of the sample, and in one case (dielectric tip) the signal on the central particle is almost lost, fading away in the background given by the neighbors.

We define here  $\Phi$  as the numerical ratio of the side peak height to the height of the central one, taken in their respective relative maxima. As a matter of fact,  $\Phi$  is markedly different

**TABLE 3. Lateral-to-Central Signal Intensity Ratio in System 2 (See Figure 2 and Figure 6) at Different Values of the Parameter  $h$** 

$h$ (nm)	10.02	10.2	11	15
$\Phi$	1.63	1.55	1.03	1.17

when changing the probe material, passing from the value of 1.03 for the Ag tip to 1.63 for the Au tip, and finally to 1.96 for the dielectric tip. Anyway, this effect, jointly with the fall of the absolute value of the field intensity detected as the tip material is changed, gives rise to a less resolved image, in which the central particle signal can be sometimes hardly detected from the background.

The same system with the Ag probe particle has been studied at different heights of the tip probe (Figure 6). The heights studied are the same used in system I (Figure 4). As for the previous system (electric field square modulus, on the left), we note that as the tip approaches the sample, a saddle-shaped signal is obtained for all the particles. Anyway, the most interesting feature here is the depression of the central peak height, that is more marked as the tip-sample distance  $h$  decreases, becoming clearly detectable for distances lower than 1 nm. Here, it is interesting to note that the  $\Phi$  value has not a monotonic behavior as a function of  $h$ : these values have been calculated and reported in Table 3. On the right side of the same figure, the scattering cross section spectra relative to the same situation have been reported. Two different tip positions (aligned along the  $z$  axis) are considered in each spectra: (1) on the central particle of the sample (continuous line); (2) on one of the four side particles (dashed-dotted line). The tip is positioned at the same height used in the calculation of the relative electric field plot (in the right). Together with these, the single-maximum spectra evaluated in absence of the tip (dashed line) is reported.

The wiggles in the scattering cross sections are due to the dielectric function used, which takes into account finite size effects as a function of wavelength as explained in a previous paper.<sup>24</sup> As expected, in absence of the tip, the system displays a broad peak splitted in two maximum, indicating that each five particles respond with a longitudinal plasmon so close to the one of others that the spectrum is not well resolved. In presence of the tip, we can roughly divide the particles of the system in two groups: tip-particle and the sample particle nearest to the tip in one group and the remaining four particles in the other. The spectrum is thus split into two signals, each associated respectively and mainly with the two groups. We note that the spectra obtained in the two different setups in the presence of the tip particle are quantitatively different; in particular, the relative intensity of the two peaks is switched, when passing from one geometry to the other. In all spectra, however, the splitting between the two maxima (when the tip is present) decreases as the tip is raised, consequently to the lower amount of coupling between the tip and the sample.

It must be borne in mind, at this point of the discussion, that we are now comparing two properties different in nature: while the electric field calculated by us is a local quantity, the scattering cross section refers to the whole system and is thus a global property. Anyway, some interesting considerations can be drawn from the comparison between these two quantities.

Here, it emerges that the plasmon peak due to the two interacting particles has a different intensity if the tip is positioned on the central particle or on the side particle, even if the position of the peak maximum is approximately the same. At the wavelength used for the near-field plots (indicated by an arrow in the graph), the scattering cross section is thus different for the two geometries with the lowest  $h$  values (Figure

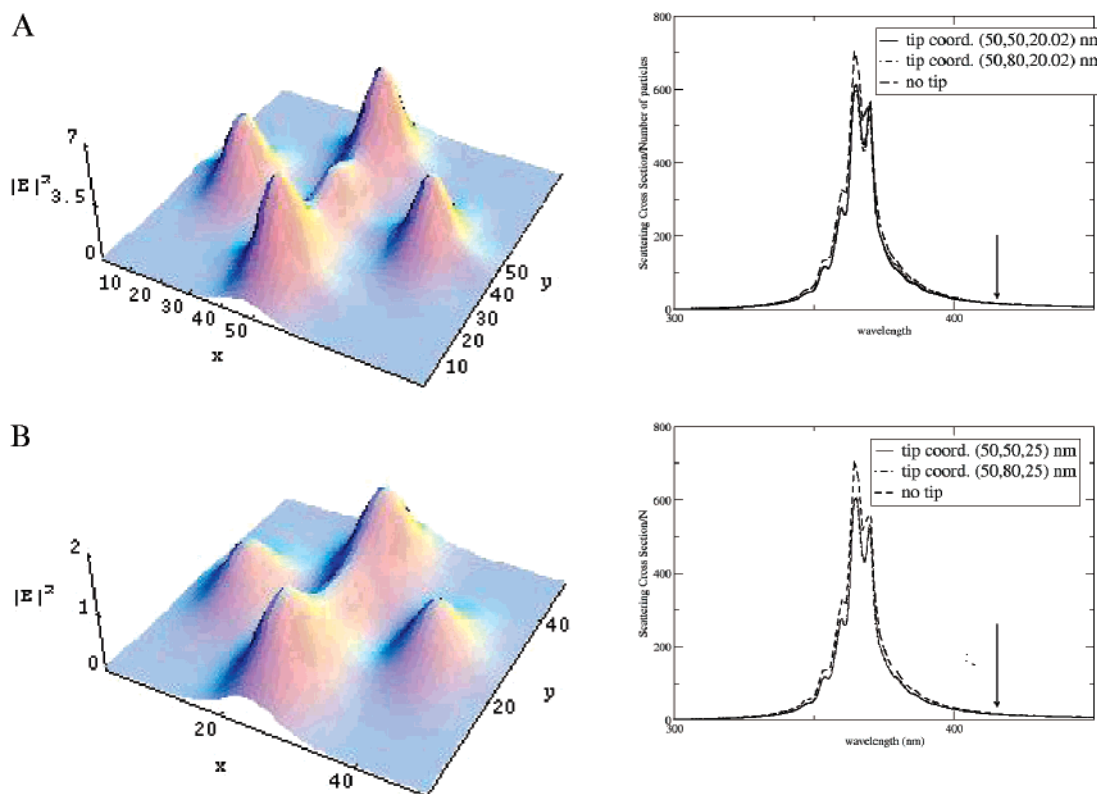


**Figure 7.** Analysis of system 2 with the tip probe ( $R_{tip} = 10$  nm) made of dielectric material at different height  $h = z_{tip} - R_{tip}$ . Left:  $|\vec{E}_{sca}(\vec{r})|^2$  plot for different  $(x,y)$  - positions. Right: Scattering cross section  $C_{sca}$  vs optical wavelength in TE polarization, in absence of the tip particle (dashed line), with the dielectric tip aligned along the  $z$  axis on the central particle (full line), or with tip aligned along the  $z$  axis on a side particle (dashed-dotted line). The arrow points on the wavelength used for near-field calculations. Key: (a)  $h = z_{tip} - R_{tip} = 10.02$  nm; (b)  $h = z_{tip} - R_{tip} = 15$  nm.



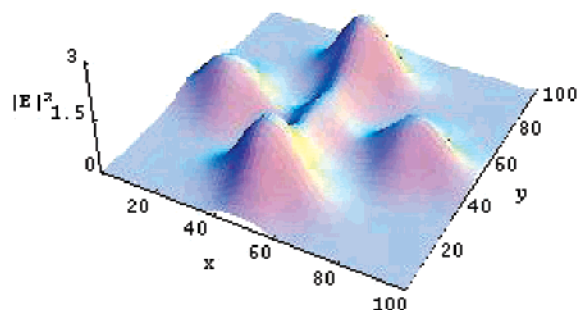


**Figure 8.**  $|\vec{E}_{\text{sca}}(\vec{r})|^2$  plot for different  $(x,y)$  positions in the  $(x,y)$  plane at height  $h = 15$  nm, for a sample constituted by five Ag particles arranged as reported in Table 1 (system 2), without tip probe.

6, parts a and b) and the cross section when the tip is on the central particle is lower than the one originated by the tip on the side particle. Conversely, at the same wavelength, no consistent differences result for the two geometries with the highest  $h$  value (Figure 6, parts c and d). This seems to be reflected, although not completely, on the relative values of the local field revealed on the central particle and on the side particle.

These considerations are, however, not sufficient to explain completely the phenomenon of signal intensity suppression on the central particle. This clearly emerges by similar calculations performed with the tip probe made of dielectric material (Figure 7). Here we limited ourselves to the two extreme values of  $h = 10.02$  nm and  $h = 15$  nm before considered. Here, the presence of the tip particle does not alter appreciably the scattering spectrum generated by the sample in absence of the tip. Only one plasmon can be clearly detected and the scattering cross section is markedly lower compared with the situation involving Ag tip at the wavelength chosen for near-field calculations. Moreover, the difference between the far-field cross sections in the two geometries of system is hardly detectable (continuous line and dotted-dashed line in Figure 7, parts a and b, on the right). This behavior of the scattering cross section is in agreement with our hypothesis that poor interaction occurs between the dielectric tip and the sample. Despite this, the local field intensity displays a suppression of the signal on the central particle without dependence from the tip height  $h$ . No detectable differences are present when comparing the local field in Figure 7, parts a and b (on the left side), between them or with the calculation showed in Figure 5c (where  $h = 1$  nm); the only difference is a predictable (and small) fall of the field amplitude as the tip is raised (no qualitative differences are found for larger values of the parameter  $h$ ). It is worth noting that the intensity ratio between the side (50,80,0) particle and the central particle signal remains almost unchanged (equal to about 2) for each  $h$  value of the tip. The poor importance of the tip on the phenomenon of the intensity suppression of the signal of the central particle is confirmed also by calculating the local field at the height of 15 nm without the tip probe (Figure 8). Even in this case we observe a marked depression of the local field on the central particle, no doubt due to the interaction between sample particles alone.

From Figures 6–8, it seems reasonable to conclude that the relative peaks height of the local field on each particle is connected to both the geometry and the chemical composition of the sample, and they can depend strongly on the sample-tip distance when the dielectric function of sample and tip are similar enough to allow a strong coupling. Anyway, a stronger difference in relative peaks height arises due to direct coupling

among the sample particles without an appreciable role of the dielectric tip at the wavelength chosen.

## Conclusions

In this work, we utilized a previously developed classical model of electromagnetic scattering from spherical nanoparticles to study the influence of coupling effects between constituents of system in near-field microscopy. Different systems, characterized by different tip materials, were simulated and their response was compared systematically.

From such compared analysis, it can be stated that the modification of collective plasmon resonances due to variation of the tip position can be very important, when a strong electromagnetic coupling can occur between tip and sample; this modification, in particular, introduces a wavelength-dependent influence on the near-field intensity, which is not connected to the sample geometry alone. It is noted, in agreement with previous calculations on a different system,<sup>13</sup> that there is no exact correspondence between near-field enhancement and far-field scattering cross section enhancement at the wavelength used for the calculations. The most important aspect, in our opinion, is nevertheless given by the fact that the differences in relative intensities are not given only by the interaction between the probe particle and the sample, but it instead can be regarded as properties of the sample even if influenced by the tip presence.

The choice of the tip material appears to be a particularly critical point deserving some comments. If a probe constituted by a material similar to the one of the sample particles appears to give very intense signals and good resolution, the utilization of a tip made of a different materials shows possible nontrivial modifications affecting the signal, which arise from the strong coupling between the involved plasmons. Contemporarily, the effect of probe height, which is found to strongly affect the signal when the tip and sample are made of the same material due to strong coupling effects, is rather negligible if the probe is constituted of a different material; this can be interesting because of the mechanical and thermal oscillation that an experimental setup is expected to undergo. In any case, a variable which is possible to tune is the wavelength of the exciting light. Due to the extreme sensitivity of the resonance plasmon to the geometry of the whole (sample + tip) system, the choice of a wavelength corresponding or near to the plasmon resonance of the system with no probe may be not the best one.

**Acknowledgment.** The authors are indebted to CNR (Progetto Finalizzato MSTA II) and Istituto Nazionale di Fisica della Materia for financial support.

## References and Notes

- (1) Papavassiliou, G. C. *Prog. Solid State Chem.* **1980**, *12*, 185.
- (2) Link, S.; El-Sayed, M. A. *J. Phys. Chem. B* **1999**, *103*, 8410.
- (3) Mishchenko, M. I.; Travis, L. D.; Lacis, A. A. *Scattering, Absorption and Emission of Light by Small Particles*; Cambridge University Press: Cambridge, U.K., 2002.
- (4) Kreibitz, U.; Vollmer, M. *Optical Properties of Metal Clusters*; Springer-Verlag: Berlin, 1995.
- (5) Quinten, M.; Kreibitz, U. *Appl. Opt.* **1993**, *32*, 6173.
- (6) Pohl, D. W.; Denk, W.; Lanz, M. *Appl. Phys. Lett.* **1984**, *44*, 651.
- (7) Betzig, E.; Harootunian, A.; Lewis, A.; Isaacson, M. *Appl. Opt.* **1986**, *25*, 1890.
- (8) Dawson, P.; de Fornel, F.; Goudonnet, J. P. *Phys. Rev. Lett.* **1994**, *72*, 2927.
- (9) Milner, R. G.; Richards, D. J. *Microsc.* **2001**, *202*, 66.
- (10) Vigoreux, J. M.; Girard, C.; Courjon, D. *Opt. Lett.* **1989**, *14*, 1039.
- (11) Denk, W.; Pohl, D. W. *J. Vac. Sci. Technol. B* **1991**, *9*, 510.
- (12) van Labeke, D.; Barchiesi, D. J. *Opt. Soc. Am. A* **1992**, *9*, 732.
- (13) Porto, J. A.; Johansson, P.; Apell, S. P.; Lopez-Rios, T. *Phys. Rev. B* **2003**, *67*, 085409.

- (14) Kawata, S.; Ohtsu, M.; Irie, M., Eds. *Nano-Optics*, Springer: Berlin, 2002.
- (15) Eah, S.-K.; Jeager, H. M.; Scherer, N. F.; Wiederrecht, G. P.; Lin, X. M. *J. Phys. Chem. B* **2005**, *109*, 11858.
- (16) Bruzzone, S.; Malvaldi, M.; Arrighini, G. P.; Guidotti, C. *J. Phys. Chem. B* **2004**, *108*, 10853.
- (17) Kottmann, J. P.; Martin, O. J. F.; Smith, D. R.; Schultz, S. *J. Microsc.* **2001**, *202*, 60.
- (18) Kelly, K. L.; Coronado, E.; Zhao, L. L.; Schatz, G. C. *J. Phys. Chem. B* **2003**, *107*, 668.
- (19) Bruzzone, S.; Malvaldi, M.; Arrighini, G. P.; Guidotti, C. *J. Phys. Chem. B* **2005**, *109*, 3807.
- (20) Gérardy, J. M.; Ausloos, M. *Phys. Rev. B* **1982**, *25*, 4204.
- (21) Bohren, C. F.; Huffman, D. R. *Absorption and Scattering of Light by Small Particles*; Wiley: New York, 1983.
- (22) Wurtz, G. A.; Hranisavljevic, J.; Wiederrecht, G. *Nano Lett.* **2003**, *3*, 1511.
- (23) Quinten, M. *Appl. Phys. B* **1998**, *67*, 101.
- (24) Bruzzone, S.; Arrighini, G. P.; Guidotti, C. *Chem. Phys.* **2003**, *291*, 125.
- (25) Ohfuti, Y.; Amanai, T. *J. Lumin.* **2000**, *87–89*, 960.
- (26) Greffet, J.-J.; Carminati, R. *Prog. Surf. Sci.* **1997**, *56*, 133.
- (27) Girard, C.; Dereux, A. *Rep. Prog. Phys.* **1996**, *59*, 657.
- (28) Xu, Y. *Appl. Opt.* **1997**, *36*, 9496.